6414 *Macromolecules* **2010**, *43*, 6414–6421
DOI: 10.1021/ma1011396

Macromolecules
ARTICLE

Dynamics of Polymer Blends of a Strongly Interassociating Homopolymer with Poly(vinyl methyl ether) and Poly(2-vinylpyridine)

Kevin A. Masser and James Runt*

Department of Materials Science and Engineering, The Pennsylvania State University, University Park, Pennsylvania 16802

Received May 21, 2010; Revised Manuscript Received July 6, 2010

ABSTRACT: The dynamics of miscible blends of poly(*p*-(hexafluoro-2-hydroxyl-2-propyl)styrene) (PolyHFS) with poly(vinyl methyl ether) (PVME) and poly(2-vinylpyridine) (P2VPy) were investigated via broadband dielectric relaxation spectroscopy (DRS). The HFS moiety forms strong intermolecular associations with proton-accepting polymers, while the steric shielding provided by the two CF_3 groups minimizes the number of self-associations. The local, glassy state relaxations of PolyHFS and PVME (or P2VPy) are suppressed in the mixtures due to the strong intermolecular hydrogen bonding. When the number of PolyHFS segments is approximately equal to the number of PVME segments, the local relaxation of PVME is undetectable by DRS. Reduced functional group accessability in P2VPy blends lessens the suppression of local relaxations. A single, broadened dynamic glass transition (α relaxation) is observed for each blend. At temperatures above the α process, an additional relaxation is observed, α*, which is assigned to the breaking and re-forming of hydrogen bonds as the chain relaxes. The temperature dependence of this process is related to the strength of the hydrogen bonding and the approximate fraction of intermolecularly associated segments.

Introduction

Hydrogen bonds have long been known to improve polymer miscibility.[1] Miscible polymer blends which do not possess specific interactions are relatively rare, miscibility being governed by van der Waals forces or the so-called χ parameter. In systems where intermolecular hydrogen bonds are formed, however, the strength of these interactions (1−10 kcal/mol) often overrides the usual driving force for phase separation, even when the non-hydrogen-bonding solubility parameters of the components suggest immiscibility. For example, copolymerizing polystyrene with just a few mole percent of poly(4-vinylphenol) (P4VPh) improves miscibility dramatically.[1]

Painter and Coleman have shown that controlled steric shielding of the OH functionality reduces the ability of a homopolymer to form self-associations.[2,3] Specifically, the equilibrium constants describing the formation of dimers (OH−OH bonds) and multimers (OH "chainlike" structures) have been found to be more than an order of magnitude lower for poly(*p*-(hexafluoro-2-hydroxyl-2-propyl)styrene) (PolyHFS, see Figure 1) than for P4VPh, while not reducing PolyHFS's ability to form intermolecular associations.[2] In fact, as we will show, the FTIR wavenumber difference between the free OH band and the intermolecularly associated OH band(s), an indication of hydrogen bonding strength,[2,4−6] is greater for PolyHFS than P4VPh, although this is not strictly due to steric shielding.

Previous studies of the dynamics of miscible polymer blends exhibiting intermolecular hydrogen bonds have found that both local[7,8] and segmental[9−11] relaxations are strongly influenced by the presence of these bonds. Strong intermolecular hydrogen bonding between proton donor and acceptor groups couples the dynamics of the component polymers, even when the dynamic asymmetry (difference in T_g between the components) is as large as 150 °C. In these systems, however, many relatively strong self (intramolecular) hydrogen bonds exist in one of the component polymers, P4VPh.[7−12] At the composition extremes, this dearth of intermolecular associations can result in two segmental relaxations, even though the blend is thermodynamically miscible.[11] This is in contrast to polymer blends lacking specific interactions, where large differences in component T_g's (> 50 °C) result in two easily discernible dynamic T_g's.[13,14]

The aim of the present study is to investigate the dynamics of miscible hydrogen-bonding polymer blends with minimized self-associations due to steric shielding. The proton donating species, PolyHFS, forms relatively strong intermolecular hydrogen bonds to the second component, either poly(vinyl methyl ether) (PVME) or poly(2-vinylpyridine) (P2VPy).

Experimental Section

Synthesis. The HFS copolymer was synthesized via free radical solution polymerization. The monomer, [1,1,1,3,3,3-hexafluoro-2-(4-vinylphenyl)propan-2-ol] (HFS), was purchased from SynQuest Laboratories. Prior to use, the HFS monomer was distilled to remove the stabilizing agent. A 50 vol % solution of 25 g of HFS in toluene was added to an air-free flask, along with 140 mg of azobis(isobutyronitrile), a free radical initiator. The mixture was freeze-dried four times to remove dissolved oxygen. An argon purge was added, and the mixture was stirred at 60 °C for 5 h, after which the reaction was terminated by the addition of chilled methanol. The polymer was reprecipitated from tetrahydrofuran (THF) into hexanes multiple times to remove impurities. Proton NMR was used to confirm the structure of the resulting polymer. Gel permeation chromatography, calibrated with polystyrene standards and using THF as the mobile phase, estimated the weight-average molecular weight of this polymer as 145 kg/mol with a polydispersity of 1.6.

PVME and P2VPy were purchased from Scientific Polymer Products, both having an approximate molecular weight of 100 kg/mol, and were purified prior to use. Each was first

*To whom correspondence should be addressed. E-mail: runt@matse.psu.edu.

 Published on Web 07/15/2010

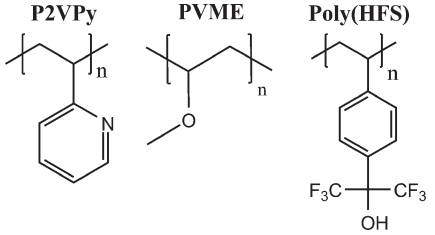

Figure 1. Repeat units of the polymers used in this study.

reprecipitated from THF into hexanes for P2VPy and warm water for PVME, then redissolved in THF, and passed through a 0.2 μm Teflon syringe filter. The homopolymers were then dried above T_g under vacuum for several days after the solvent had been removed. The structures of the polymers used in this study are shown in Figure 1.

Blend Preparation. All blends were prepared by mixing the appropriate amounts of each component with THF to form dilute solutions (2−5%). After filtering with a 0.2 μm Teflon syringe filter, the blends were dried above T_g under vacuum with a cold trap for several days to remove solvent and moisture. Unlike P4VPh blends,[8,15] PolyHFS does not readily form a complex with P2VPy in THF. No precipitate was formed during mixing or subsequent drying of the P2VPy blends.

Differential Scanning Calorimetry (DSC). Thermal characteristics were measured using a Seiko DSC220CU DSC. Each sample was run using the following procedure: heat at 10 deg/min to $T_g + 50$ °C, cool at 10 deg/min to $T_g - 50$ °C, and heat to $T_g + 50$ °C at 10 deg/min. The temperature was held for 5 min at each extreme ($T_g \pm 50$ °C) for 5 min before continuing. T_g was taken as the midpoint of the heat capacity step from the second heating scan.

Fourier Transform Infrared Spectroscopy (FTIR). FTIR was conducted on a Nicolet 6700 with an attached dry air purge. A minimum of 100 scans were averaged with a wavenumber resolution of 2. To verify the stability of the blends at elevated temperatures, temperature-dependent FTIR was conducted with an attached heating cell from room temperature to temperatures above those used in dielectric measurements. Heating and cooling scans were performed to ensure phase separation and degradation did not occur.

Broadband Dielectric Relaxation Spectroscopy (DRS). Samples were prepared for DRS measurements by solution casting thin films from THF; 50−200 μm (±3%) thick, and 30 mm in diameter. Brass electrodes were placed onto the surfaces of the film to ensure good electrical contact, usually 25 and 30 mm for the upper and lower surfaces, respectively. Silica fibers, 50 μm in diameter, were pressed into the film with the electrodes to maintain the sample thickness. DRS measurements were performed on a Concept 40 system from Novocontrol GmbH, over the frequency range of 10 mHz−10 MHz. Temperature was controlled by a Quatro temperature control system which heats evaporated liquid nitrogen with a precision of greater than ±0.1 °C. All blends were measured over the temperature range of −140 °C to well above the calorimetric T_g. After DRS measurements, films were redissolved in good solvent to ensure cross-linking did not occur at elevated temperatures.

The imaginary part (loss) of the complex dielectric function ($\varepsilon^*(\omega) = \varepsilon'(\omega) - i\varepsilon''(\omega)$) was fit using one or more empirical Havriliak−Negami equations:[16]

$$\varepsilon''(\omega) = -\sum_{r=1}^{n} \mathrm{Im}\frac{\Delta\varepsilon_r}{(1+(i\omega\tau_{\mathrm{HN}r})^{\alpha_r})^{\gamma_r}} + \frac{\sigma_0}{(\omega\varepsilon_0)^s} \qquad (1)$$

$\Delta\varepsilon$ is the strength of the relaxation and is related to the number of dipoles contributing to the dispersion.[17−19] ω and τ_{HN} are the angular frequency and relaxation time, respectively. α and γ are the broadening and high-frequency asymmetry parameters, respectively. The second term of eq 1 describes the dc conductivity, a result of motions of impurity ions. σ_0 is the frequency-independent (dc) conductivity, ε_0 is the permittivity of free space, and the parameter s relates to the type of conduction present.[19]

Table 1. Thermal Characteristics of the Blends Studied (ΔT_g Is the Breadth of the Transition)

Blend	mol % HFS (±1%)	wt % HFS (±1%)	T_g (±3 °C)	ΔT_g (±5 °C)
P2VPy	0	0	100	10
	12	25	110	20
	28	50	137	21
	54	75	149	15
	78	90	138	14
PVME	0	0	−26	5
	7	25	−11	24
	18	50	9	22
	38	75	61	27
	69	90	80	13
	100	100	125	11

At temperatures above T_g, the motions of impurity ions begin to dominate the dielectric loss, often obscuring dipolar relaxations. With the exception of the phenomenon of electrode polarization, motions of ionic impurities do not manifest themselves in the dielectric constant (ε').[19] The fundamental Kramers−Kronig relationship states the dielectric loss and the dielectric constant contain the same information, so one can be calculated from the other. Since a cumbersome numerical approximation is necessary for the Kramers−Kronig relationship to be applied,[20] the derivative of the dielectric constant was used. Wübenhorst et al. have shown that the derivative of the real part of the complex permittivity, or the dielectric constant, is a good approximation of the conductivity-free dielectric loss:[21,22]

$$\varepsilon''_{\mathrm{der}} = -\frac{\pi}{2}\frac{\partial\,\varepsilon'(\omega)}{\partial \ln\omega} \approx \varepsilon'' \qquad (2)$$

The usefulness of this formalism is its ability to not only remove dc conductivity from the dielectric loss, but it has also been shown to partially resolve overlapping peaks.[23] As long as the appropriate fitting function is used (see eq 7 of ref 23) in the analysis of the data, the derivative formalism yields results identical to the raw dielectric loss, with the added benefit of being able to deconvolute dipolar response from ion motion.[23,24]

From the relaxation time (τ_{HN}) determined by fitting eq 1 to the dielectric loss data, or the appropriate function for the derivative loss, the frequency maxima can be calculated from the following:

$$f_{\max} = \frac{1}{2\pi\tau_{\mathrm{HN}}}\left[\frac{\sin\left(\frac{\alpha\pi}{2+2\gamma}\right)}{\sin\left(\frac{\alpha\gamma\pi}{2+2\gamma}\right)}\right]^{1/\alpha} \qquad (3)$$

The parameters in eq 3 are the same as those in eq 1.

Results and Discussion

DSC. All blends were found to exhibit a single calorimetric glass transition (see Table 1).

At select compositions, the T_g of some P2VPy blends is between 12 and 24 degrees *higher* than the high-T_g component, a result of the strong intermolecular coupling. Figure 2 displays the T_g's of the blends as a function of composition.

FTIR. FTIR spectroscopy has been shown to be sensitive to the various states of the OH functionality (nonbonded and various types of bonded), exhibiting a variety of absorption bands in the spectral region from 3000 to 3650 cm^{-1}.[1] For the HFS functionality, bands at 3602 and 3520 cm^{-1} have been

assigned as nonbonded or "free" OH groups and dimers and multimers, respectively.[2] It has been shown that as a second hydrogen-bonding species is blended with the HFS functionality, an additional band (or bands) appeared, indicating the presence of intermolecular hydrogen bonds. More importantly, it was found that the wavenumber difference between the free OH band and the intermolecular association band is indicative of the strength of the hydrogen bond.[2,4,5] If the absorptivity coefficient of the band in question is unknown, however, as is the case here, only a qualitative assessment of the hydrogen bonding strength is possible.[1,2]

Shown in Figure 3a,b is the OH stretching region of the blends. Both PVME and P2VPy blends exhibit strong intermolecular associations, evidenced by the appearance of new absorption bands at ~3200 and ~2900 cm^{-1} for the PVME and P2VPy blends with PolyHFS, respectively. The relative wavenumber shifts of both the PVME and P2VPy blends suggests the HFS functionality forms slightly stronger intermolecular associations in these systems compared to poly(4-vinylphenol) (P4VPh).[1] In blends of PVME with P4VPh,[6,25] bands associated with intermolecular associations were found to shift by no more than 350 cm^{-1}, whereas the wavenumber shift in the PVME blends examined here ranges from 350 to 450 cm^{-1}. For P2VPy blends with P4VPh, a complex was formed, and the wavenumber shift arising from the resulting associations was found to be ~600 cm^{-1}.[15] As shown in Figure 3b, the band associated with intermolecular associations in the P2VPy blends is centered at ~700 cm^{-1} below the "free" OH band at 3602 cm^{-1}, 100 cm^{-1} more than in analogous P4VPh blends. An exact value of the wavenumber shift in these blends is difficult to determine, however, due to the occurrence of the aliphatic and aromatic C−H stretching vibrations in the region from 2800 to 3100 cm^{-1}.[15]

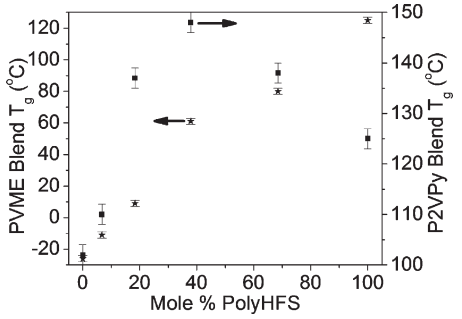

Figure 2. Glass transition temperatures of the blends examined here: PVME (★) blend T_g's are plotted on the left axis; P2VPy (■) blend T_g's on the right.

Broadband Dielectric Relaxation Spectroscopy. *Local Relaxations.* The well-known β relaxation of PVME has been attributed to rotations of PVME's pendant methoxy group,[13] and the temperature dependence of this and similar glassy state processes can be modeled with an Arrhenius equation.

$$f_{max}(T) = f_0 \exp\left(-\frac{E_a}{RT}\right) \quad (4)$$

In eq 4, R is the universal gas constant, E_a is the activation energy, and f_0 is the frequency prefactor. It is expected that formation of hydrogen bonds between the PVME methoxy group and the HFS OH group should suppress this relaxation, assuming sufficient numbers of hydrogen bonds are present, as seen in a previous study of intermolecularly hydrogen-bonding blends.[8] As shown in Figures 4a and 5a, the temperature dependence of this relaxation is unaffected in the blends, maintaining the same relaxation time as a function of temperature and an activation energy of 25 ± 2 kJ/mol. The dielectric strength, however, as shown in Figure 5a is strongly reduced, beyond what is expected from simply diluting the number of segments. This is shown more clearly in Figure 5b, where the dielectric loss is scaled by the mole fraction of PVME in the system. A reduction in the number of dipoles contributing to the relaxation process is expected, since a fraction of the remaining PVME methoxy functional groups will be rotationally restricted due to hydrogen bonds formed with the HFS OH groups. At the highest concentration of the HFS homopolymer (69 mol %), the local relaxation of PVME is completely suppressed. This reduction in strength is in contrast to a previous study of blends of PVME and a strongly interassociating copolymer.[26] It was shown that the relaxation time and strength of the PVME β process were unaffected by blending, beyond the effects of simply diluting the number of PVME segments, which was attributed to the relatively low number of HFS segments (14 mol %) present in the copolymer.

In contrast to the local motions of PVME, the local process of the HFS homopolymer does exhibit a change in activation energy (from 54 to 37 (±2) kJ/mol) upon blending with PVME. The lowering of the activation energy of the PolyHFS local process in the 69 mol % blend is most likely due to the change in local environment from the neat HFS homopolymer, similar to what is observed in some plasticized systems.[27,28] It is unclear, however, why the PVME local process does not exhibit a change in activation energy in

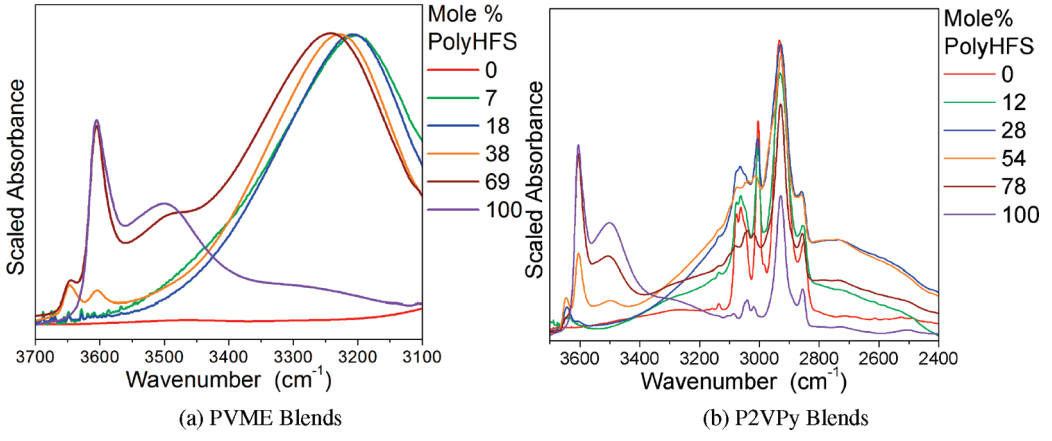

Figure 3. OH stretching region for blends of the HFS homopolymer with (a) PVME and (b) P2VPy.

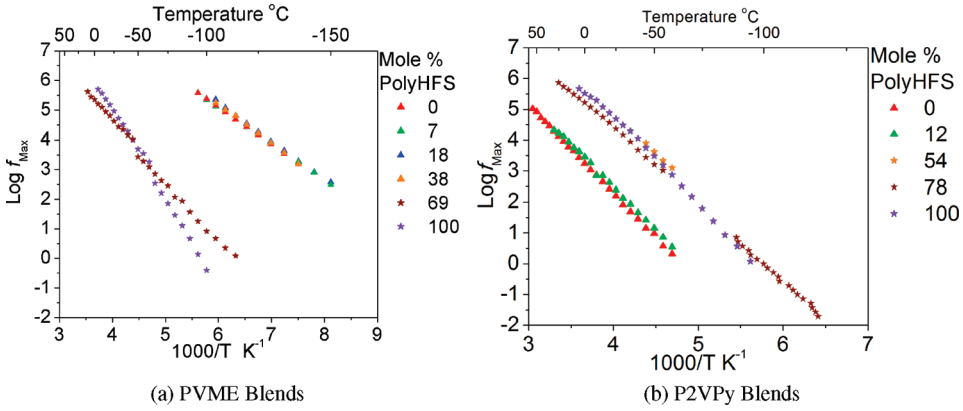

Figure 4. Arrhenius representation of the β relaxations of the blends of PVME (a) and P2VPy (b). The relaxation times of the local process of PVME and P2VPy (▲) and of PolyHFS (★) are shown.

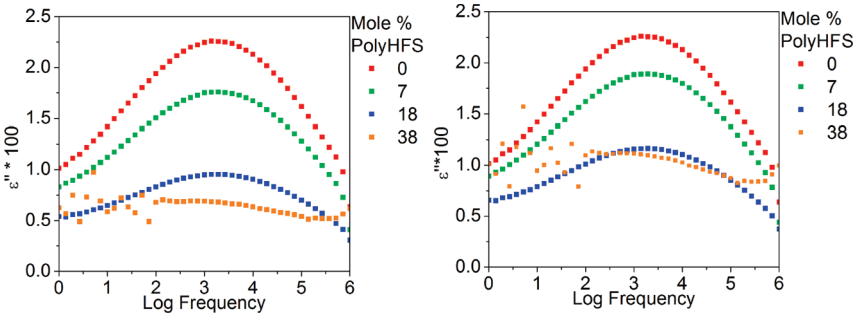

Figure 5. Dielectric loss for the PVME−PolyHFS blends at −140 °C (a) and scaled by the mol % PVME (b).

the blends, as seen in antiplasticized blends,[29] or why the temperature dependence of the PolyHFS β process is unaffected in the P2VPy blends. The 69 mol % blend is the only PVME blend exhibiting a strong, free OH peak at 3602 cm^{-1} (see Figure 3a). The 38 mol % blend exhibits a small free OH peak, but it is unlikely the sensitivity of DRS is sufficient to adequately resolve a relaxation resulting from such a small number of free functional groups. As shown in Figure 4a, the local relaxation of PolyHFS is detectable only when it is the majority component of the blend. In a similar study of blends of PVME and an HFS−dimethylbutadiene copolymer,[26] the copolymer β process is only present in the neat copolymer and has a temperature dependence similar to that of the PolyHFS homopolymer, suggesting this relaxation is associated with the motion of the HFS functional group.

Scaling the loss in the P2VPy blends (Figure 6) is not as straightforward as the PVME blends (Figure 5b), since the local process of P2VPy and PolyHFS overlap. It is, however, clear that local motions are suppressed due to the strong hydrogen bonds formed. Of interest are the 28 and 78 mol % PolyHFS blends (blue and brown squares, respectively, in Figure 6). There is a molar excess of P2VPy in the 28 mol % blend, yet the local relaxations are suppressed more strongly than at any other blend composition. This can be attributed to the fraction of segments which are hydrogen bonded to each other and the fact that the volume fractions of P2VPy and PolyHFS are approximately equal at this composition. The P2VPy β process is present in the 78 mol % PolyHFS blend with P2VPy, even though there is a large molar excess of PolyHFS. It is clear from these results that the reduced functional group accessability in these blends plays an important role.

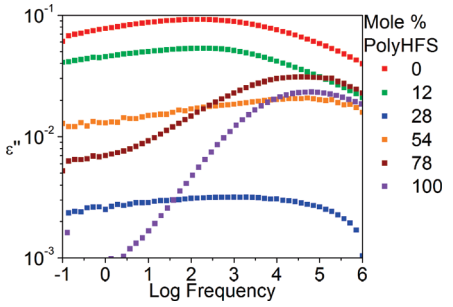

Figure 6. Dielectric loss at −30 °C for the P2VPy blends.

Various studies, including theoretical calculations and measurements, have shown that at nearly any composition some fraction of functional groups capable of participating in a hydrogen bond will be free.[1,2,30] Examination of Figure 3b reveals that the 28 mol % blend is nearly devoid of free OH groups, while the 54 mol % blend exhibits not only free OH groups but also self-associations, evidenced by a small band at 3520 cm^{-1}. This underlines the effect of functional group accessability on the ability of two polymers to form associations. Since both PolyHFS and P2VPy have "free" functional groups in the 54 mol % blend, the local relaxation of both polymers should be present. Note that in Figure 6 a very small peak in the 28 mol % blend related to the local relaxation of P2VPy does appear to be present, but its intensity is too low for its relaxation behavior to be accurately modeled. As noted earlier, since the absorptivity coefficients of the self-association bands at ~3520 cm^{-1} are unknown, quantitative values of the fraction of hydrogen-bonded segments cannot be obtained.

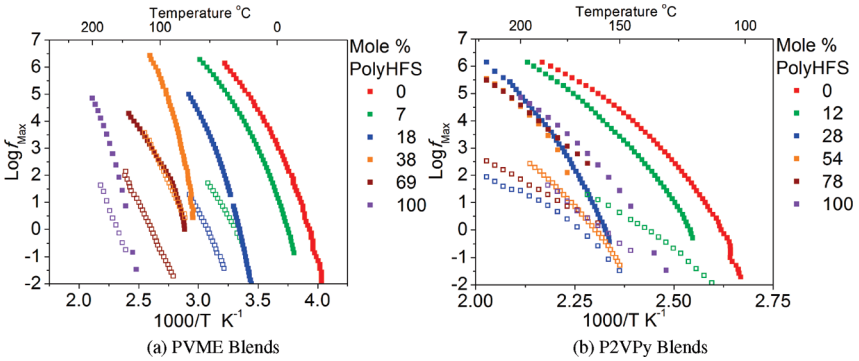

Figure 7. Frequency maxima of the segmental (■) and α* (□) relaxations for the PVME (a) and the P2VPy (b) blends.

Segmental Relaxations. The segmental (α) relaxation, or dynamic T_g, is observable in the experimental window at temperatures above the DSC-determined T_g and involves micro-Brownian motion of several repeat units.[19,31] The temperature dependence of the α relaxation time can be modeled with a Vogel−Fulcher−Tamman (VFT) equation.[19]

$$f_{max}(T) = f_0 \exp\left(-\frac{B}{T - T_0}\right) \quad (5)$$

f_0 is the exponential prefactor or the relaxation frequency at infinite temperature. B is related to the fragility of the system,[32] which can also be written as DT_0.[24,33] T_0 is the Vogel temperature or the temperature at which eq 5 diverges. The resulting VFT fit parameters obtained from fitting the segmental relaxation frequencies (see Figure 7a,b) are listed in Table 2.

All blends exhibited a single segmental relaxation, indicative of dynamic homogeneity, or complete miscibility. In blends containing relatively low concentrations of PVME, the segmental relaxation was broadened, expected due to the large dynamic asymmetry of the components. The 69 mol % PolyHFS blend with PVME could not be accurately modeled with a VFT function. Although exhibiting a single α relaxation and an α* relaxation (vide infra), the blend is likely undergoing phase separation, since the experimental temperatures are near the degradation temperature of PVME.

The steepness (or fragility) index of a glass former is defined as

$$m = \left.\frac{\partial \log x}{\partial(T_g/T)}\right|_{T=T_g} = \frac{BT_g}{\ln(10)(T_g - T_0)^2} \quad (6)$$

x is a dynamic variable such as viscosity or relaxation time ($\tau = 1/2\pi f$) as in the case of this study, B and T_0 are the same as eq 5.[32] A "fragile" glass-former (higher value of m) is one with a greater deviation from Arrhenius behavior or one whose slope of the segmental relaxation time/frequency at $T = T_g$ is higher. Note that fragility was calculated with the VFT-determined T_g ($\tau_{max} = 100$ s), not the calorimetric T_g.

Although not explicitly stated by Adam and Gibbs, the fragility can be related to the configurational entropy available to the system.[34] It was shown that the height of the potential energy barrier per monomer unit ($\Delta\mu$) was higher for hydrogen-bonding systems, owing to the increased intermolecular coupling. This increase in $\Delta\mu$ implies an increase in the steepness index (see eqs 28 and 29′ of ref 34) or fragility.

A correlation between the fragility and the size of a cooperatively rearranging region (CRR) has been proposed.[35] As the degree of intermolecular coupling is increased, the configurational entropy available to the system decreases, $\Delta\mu$ and the CRR increase, and the fragility of the system

Table 2. VFT Fitting Parameters for the Segmental Relaxation[a]

Blend	mol % PolyHFS (±1%)	log[f_0 (Hz)] (±1)	B (±10 K)	T_o (±3 °C)	VFT-T_g (±3 °C)	Fragility (±10)
P2VPy	0	11	1660	44	95	102
	12	11	1590	58	107	109
	28	11	1370	103	146	135
	54	11	1430	104	149	130
	78	11	1860	74	133	94
PVME	0	12	1310	−68	−28	87
	7	11	1380	−59	−17	87
	18	11	1310	−28	12	101
	38	11	880	28	56	160
	69					
	100	11	1920	63	124	89

[a] VFT-T_g is defined as the temperature where the relaxation time of the segmental process is 100 s. Fragility values calculated using the VFT-T_g.

increases. As temperature increases, the hydrogen-bonding strength as well as the number of intermolecular associations decreases,[1] and the system's entropy increases. Since hydrogen-bonding strength decreases with increasing temperature, the higher the blend T_g, the weaker the intermolecular associations of that blend at T_g. Assuming two blends have a similar number of intermolecular hydrogen bonds, one would expect the system with the higher T_g to have a stronger temperature dependence of the segmental relaxation; the CRR size decreases rapidly, and the number of configurations available to the system (entropy) increases rapidly with temperature. Examination of the blend FTIR spectra (Figure 3a,b) shows that the 28 mol % PolyHFS blend with P2VPy and the 38 mol % PolyHFS blend with PVME possess the highest fraction (qualitatively) of *intermolecularly* associated segments. This is evidenced by a small free OH peak at 3602 cm^{-1} in both systems, meaning nearly every HFS segment in both blends is intermolecularly associated and supported by the behavior of the local processes of these blends (orange and blue points in Figures 5a and 6, respectively), being the most strongly suppressed. These blends exhibit the highest fragilities, over 70 higher than the neat components in the case of PVME blends and 46 in P2VPy blends. It should be noted that due to the strong overlap of the α* and α processes in the P2VPy blends, the relaxation behavior of the α relaxation of the 54 and 78 mol % PolyHFS blends with P2VPy could not be modeled accurately near T_g. The fragilities of these two blends should therefore be treated with caution and may in fact be much larger in the 54 mol % blend, but the observed trends in the calculated fragility values agree well with the observed behavior of the local relaxations and the FTIR results.

Interestingly, the 38 mol % PolyHFS blend with PVME exhibits a fragility which is 25 *higher* than the most fragile

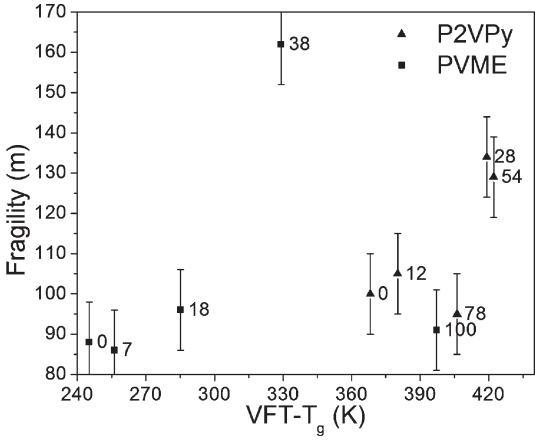

Figure 8. Fragility parameter (m) as a function of T_g for the P2VPy blends (▲) and the PVME blends (■). The PolyHFS mol % of each blend is listed beside the corresponding data point.

P2VPy blend. This appears to be at odds with the strength of the hydrogen bonding in both blend systems (P2VPy≫ PVME) and the expected intermolecular coupling. Inspection of the blend FTIR (Figure 3a,b) and the local relaxations (Figures 5a and 6) suggests that the fraction of hydrogen-bonded segments (degree of intermolecular coupling) is greater in the 38 mol % PolyHFS blend with PVME than in any other blend (P2VPy or PVME). A small free OH band (see Figure 3a) and an almost complete suppression of the PVME local process (Figure 5a) support the assertion that the fraction of hydrogen-bonded segments is highest in this blend and should therefore have the highest fragility (see Figure 8) of the systems studied. The fragilities of the blends reported here suggest that, at least in the case of intermolecularly hydrogen-bonded polymer blends, the fragility is dictated not by T_g,[36] but by the degree of intermolecular coupling.

The trends in fragilities exhibited by these systems are in qualitative agreement with cross-linked systems, which exhibit increased fragility as the degree of cross-linking is increased,[37−39] and with recent studies on the effects of plasticization.[40,41] In a previous study of PVME blends with P4VPh, similar trends were observed in the calculated fragilities; the fragility increased with the fraction of intermolecularly associated segments.[11] The fragility values were somewhat lower than those reported here due to the relatively strong self-associations which exist in P4VPh, which result in a lower degree of intermolecular coupling than in the blends examined here, and the stronger hydrogen bonds formed by PolyHFS versus P4VPh.

It is generally accepted that the dynamic asymmetry ($T_{g,A} - T_{g,B}$) plays a major role in the resulting blend dynamics.[1f,13,42] A greater difference in the component T_g's results in a broadened blend T_g. In the systems examined here, however, the calorimetric transition breadth and the segmental relaxation breadth of the PVME blends ($T_{g,PolyHFS} - T_{g,PVME} = 151$) are roughly the same as the P2VPy blends ($T_{g,PolyHFS} - T_{g,P2VPy} = 25$), which have a much smaller difference in component T_g's. This suggests that in the case of hydrogen-bonded polymer blends the degree of intermolecular associations and the functional group accessability are the important factors in determining the relaxation behavior, not the dynamic asymmetry.

High Temperature Relaxations. At temperatures above and frequencies below the segmental relaxations of the blends, each blend exhibited an additional relaxation (Figure 10a,b)[22,43−46] which was nearly Debye (from the derivative HN equation: $\alpha = 0.8-0.9, \gamma = 1$). This process is not related to the phenomenon of electrode polarization,

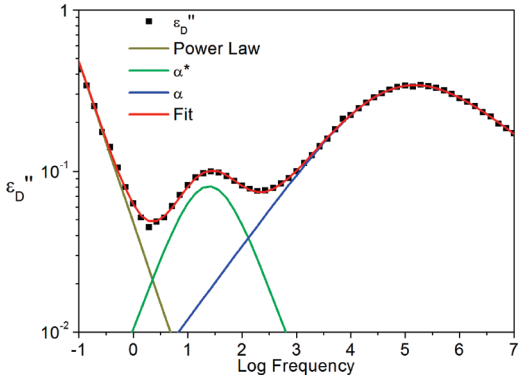

Figure 9. Representative fit of the relaxations above T_g.

which is observed at still higher temperatures and whose magnitude in the derivative dielectric loss is significantly greater than this relaxation. In previous studies of functionalized polybutadienes,[44,45] a similar process was observed with an activation energy (E_a from eq 4) of ~110 kJ/mol and an Arrhenius prefactor (f_0 from eq 4) of 10^{27} Hz were found for this α* process, significantly higher than for a local relaxation. Fitting eq 4 to the PVME α* data yields an activation energy of 206 ± 20 kJ/mol, higher than that of Muller et al., and an Arrhenius prefactor of $10^{27\pm1}$ Hz, in agreement with the findings of Muller et al.,[44] suggesting this process is of similar origin: the breaking and re-forming of hydrogen bonds as segmental relaxation occurs. See Figure 9 for a representative fit to this high-temperature process. The differences in activation energies between the findings of Muller et al. and this study are likely due to the differences in the numbers and types of hydrogen bonds present in the systems. The increased scatter, and somewhat VFT-like behavior of the α* process in the P2VPy blends is due to the much stronger overlap of this process with the α relaxation.

In addition to hydrogen-bonded systems, relaxations due to the breaking and re-forming of associations at elevated temperatures have been seen in ionomers, in both mechanical[47] and dielectric spectroscopy,[48] suggesting this relaxation may be an inherent feature of systems possessing strong associations.

Small and wide-angle X-ray scattering (not shown) do not indicate the presence of a second phase, so it is unlikely this relaxation is due to interfacial polarization, the buildup of charge at the interface of inhomogeneous systems (Maxwell−Wagner−Sillars interfacial polarization, see Chapter 13 of ref 19). At low temperatures ($T_{g,DSC} - 5 < T < T_{g,DSC} + 10$) in the P2VPy blends, the α* relaxation occurs at higher frequencies than the α relaxation. Since the interfacial polarization phenomena requires mobile charges ($T > T_g$), the α* process would not be present at these temperatures if this relaxation were related to interfacial polarization. Note that interfacial polarization requires mobile charges in only one phase.[19] If these systems were phase separated, the relative magnitudes of the α and α* relaxations suggest the α* process would be from the hydrogen-bonded segments and should have a higher T_g. The α* process is Arrhenius and extrapolates to temperatures below the α, strongly suggesting this process is not a result of interfacial polarization.

The occurrence of the α* relaxation at frequencies above (and temperatures below) the α relaxation near T_g suggests that this relaxation, the breaking and re-forming of hydrogen bonds, must occur before segmental level relaxation can occur in some of the blends. This observation is in line with the observed trends in the blends' T_g's and the number and

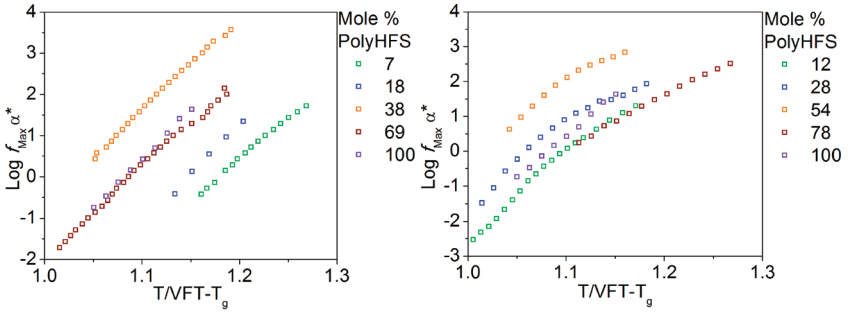

Figure 10. Frequency maxima of the α* process for the PVME (a) and the P2VPy (b) blends versus temperature scaled by the temperature at which $\tau_{Max} = 100$ s (VFT-T_g).

strengths of the hydrogen bonds. The 7 and 18 mol % PolyHFS blends with PVME possess relatively few intermolecular associations, so segmental level motion can occur without the breaking of these associations. As the fraction of intermolecularly associated segments approaches 1, segmental level motion cannot occur without breaking intermolecular associations (the α* relaxation). In the case of the P2VPy blends, the hydrogen bonds are far stronger than the PVME blends (Figure 3a,b), so higher temperatures, in some cases greater than the T_g of the blend components, would be required to break enough hydrogen bonds for segmental level relaxation to occur.

This also explains the presence of the α* relaxation in the HFS homopolymer. Although possessing few self-associations,[2] some self-associations are present. In Figure 7a,b, the relaxation time of the PolyHFS α* extrapolates to time scales shorter than that defined for T_g (100 s), again suggesting that hydrogen bonds dictate the T_g of this homopolymer.

Conclusions

The effects of strong intermolecular associations on the dynamics of miscible hydrogen-bonding polymer blends of PolyHFS with PVME and P2VPy have been explored. Minimized self-associations in PolyHFS result in blends with a greater degree of intermolecular coupling compared to analogous P4VPh blends.

Intermolecular coupling was found to strongly influence local relaxations. Strong suppression of the local relaxation of each component was observed and correlated well with the hydrogen-bonding behavior observed in FTIR spectroscopy. In PVME blends, the suppression of local motions scaled well with the blend composition. In P2VPy blends, however, the suppression of the local motions was governed not simply by the ratio of functional groups, but by functional group accessability.

A single calorimetric and dynamic T_g was observed for each blend. The temperature dependence of the segmental relaxation times strongly depends on the numbers and strengths of hydrogen bonds in the system. As the molar ratio of P2VPy to PolyHFS approaches 1, the T_g (and the segmental relaxation) occurs at temperatures above those of the component polymers. The fragility of each system is strongly correlated to the intermolecular hydrogen bonding. The 38 mol % PolyHFS blend with PVME exhibited the highest fragility because it possessed the largest fraction of intermolecularly associated segments (for the PVME blends).

The α* relaxation was present in the DRS spectra of all blends and only observable in the conductivity free loss (ε''_{der}), and its temperature dependence follows the strength and number of hydrogen bonds. Future studies will investigate these effects in systems where the fraction of intermolecular associations can be quantified.

Acknowledgment. The authors thank the National Science Foundation for financial support of this research through DMR-0907139 and Dr. Daniel Fragiadakis, Dr. Paul Painter, and Hanqing Zhao for helpful discussions.

References and Notes

(1) Coleman, M. M.; Graf, J.; Painter, P. C. *Specific Interactions and the Miscibility of Polymer Blends*, 1st ed.; Technomic Publishing Co.: Lancaster, 1991.
(2) Yang, X. M.; Painter, P. C.; Coleman, M. M.; Pearce, E. M.; Kwei, T. K. *Macromolecules* **1992**, *25*, 2156–2165.
(3) Coleman, M. M.; Pehlert, G. J.; Yang, X. M.; Stallman, J. B.; Painter, P. C. *Polymer* **1996**, *37*, 4753–4761.
(4) Drago, R. S.; Epley, T. D. *J. Am. Chem. Soc.* **1969**, *91*, 2883–2890.
(5) Drago, R. S.; Obryan, N.; Vogel, G. C. *J. Am. Chem. Soc.* **1970**, *92*, 3924–3929.
(6) Serman, C. J.; Xu, Y.; Painter, P. C.; Coleman, M. M. *Polymer* **1991**, *32*, 516–522.
(7) Zhang, S. H.; Runt, J. *J. Polym. Sci., Part B: Polym. Phys.* **2004**, *42*, 3405–3415.
(8) Zhang, S. H.; Painter, P. C.; Runt, J. *Macromolecules* **2004**, *37*, 2636–2642.
(9) Zhang, S. H.; Painter, P. C.; Runt, J. *Macromolecules* **2002**, *35*, 8478–8487.
(10) Zhang, S. H.; Painter, P. C.; Runt, J. *Macromolecules* **2002**, *35*, 9403–9413.
(11) Zhang, S. H.; Jin, X.; Painter, P. C.; Runt, J. *Polymer* **2004**, *45*, 3933–3942.
(12) Zhang, S. H.; Jin, X.; Painter, P. C.; Runt, J. *Macromolecules* **2002**, *35*, 3636–3646.
(13) Urakawa, O.; Fuse, Y.; Hori, H.; Tran-Cong, Q.; Yano, O. *Polymer* **2001**, *42*, 765–773.
(14) Colmenero, J.; Arbe, A. *Soft Matter* **2007**, *3*, 1474–1485.
(15) Lee, J. Y.; Painter, P. C.; Coleman, M. M. *Appl. Spectrosc.* **1986**, *40*, 991–994.
(16) Havriliak, S.; Negami, S. *J. Polym. Sci., Part C: Polym. Symp.* **1966**, 99–117.
(17) Onsager, L. *J. Am. Chem. Soc.* **1936**, *58*, 1486–1493.
(18) Kirkwood, J. G. *J. Chem. Phys.* **1939**, *7*, 911–919.
(19) Kremer, F.; Schonhals, A. *Broadband Dielectric Spectroscopy*, 1st ed.; Springer-Verlag: New York, 2003.
(20) Steeman, P. A. M.; vanTurnhout, J. *Colloid Polym. Sci.* **1997**, *275*, 106–115.
(21) Wübbenhorst, M.; vanKoten, E. M.; Jansen, J. C.; Mijs, W.; vanTurnhout, J. *Macromol. Rapid Commun.* **1997**, *18*, 139–147.
(22) Wübbenhorst, M.; van Turnhout, J.; Folmer, B. J. B.; Sijbesma, R. P.; Meijer, E. W. *IEEE Trans. Dielectr. Electr. Insul.* **2001**, *8*, 365–372.
(23) Wübbenhorst, M.; van Turnhout, J. *J. Non-Cryst. Solids* **2002**, *305*, 40–49.
(24) Fragiadakis, D.; Dou, S.; Colby, R. H.; Runt, J. *J. Chem. Phys.* **2009**, *130*, 0649071–06490711.
(25) Zhang, S. H.; Jin, X.; Painter, P. C.; Runt, J. *Macromolecules* **2003**, *36*, 5710–5718.
(26) Masser, K. A.; Runt, J. *Macromol. Symp.* **2009**, *279*, 221–227.
(27) Ngai, K. L.; Rendell, R. W.; Yee, A. F. *Macromolecules* **1988**, *21*, 3396–3401.

(28) Atorngitjawat, P.; Klein, R. J.; McDermott, A. G.; Masser, K. A.; Painter, P. C.; Runt, J. *Polymer* **2009**, *50*, 2424–2435.
(29) Ngai, K. L.; Rendell, R. W.; Yee, A. F.; Plazek, D. J. *Macromolecules* **1991**, *24*, 61–67.
(30) Zhang, S. H.; Runt, J. *J. Phys. Chem. B* **2004**, *108*, 6295–6302.
(31) Williams, G. *Macromol. Symp.* **2009**, *286*, 1–19.
(32) Angell, C. A. *Science* **1995**, *267*, 1924–1935.
(33) Richert, R.; Angell, C. A. *J. Chem. Phys.* **1998**, *108*, 9016–9026.
(34) Adam, G.; Gibbs, J. H. *J. Chem. Phys.* **1965**, *43*, 139–146.
(35) Saiter, A.; Saiter, J. M.; Grenet, J. *Eur. Polym. J.* **2006**, *42*, 213–219.
(36) McKenna, G. B. *J. Non-Cryst. Solids* **2009**, *355*, 663–671.
(37) Alves, N. M.; Ribelles, J. L. G.; Tejedor, J. A. G.; Mano, J. F. *Macromolecules* **2004**, *37*, 3735–3744.
(38) Kalakkunnath, S.; Kalika, D. S.; Lin, H. Q.; Freeman, B. D. *Macromolecules* **2005**, *38*, 9679–9687.
(39) Casalini, R.; Roland, C. M. *J. Polym. Sci., Part B: Polym. Phys.* **2010**, *48*, 582–587.
(40) Stukalin, E. B.; Douglas, J. F.; Freed, K. F. *J. Chem. Phys.* **2009**, *131*, 1149051–11490511.
(41) Stukalin, E. B.; Douglas, J. F.; Freed, K. F. *J. Chem. Phys.* **2010**, *132*, 0845041–08450411.
(42) Leroy, E.; Alegria, A.; Colmenero, J. *Macromolecules* **2003**, *36*, 7280–7288.
(43) Leibler, L.; Rubinstein, M.; Colby, R. H. *Macromolecules* **1991**, *24*, 4701–4707.
(44) Müller, M.; Stadler, R.; Kremer, F.; Williams, G. *Macromolecules* **1995**, *28*, 6942–6949.
(45) Müller, M.; Kremer, F.; Stadler, R.; Fischer, E. W.; Seidel, U. *Colloid Polym. Sci.* **1995**, *273*, 38–46.
(46) Müller, M.; Seidel, U.; Stadler, R. *Polymer* **1995**, *36*, 3143–3150.
(47) Douglas, E. P.; Waddon, A. J.; Macknight, W. J. *Macromolecules* **1994**, *27*, 4344–4352.
(48) Atorngitjawat, P.; Klein, R. J.; Runt, J. *Macromolecules* **2006**, *39*, 1815–1820.